

Analysis on Simulation of Quasi-Steady Molecular Statics Nanocutting Model and Calculation of Temperature Rise During Orthogonal Cutting of Single-Crystal Copper

Zone-Ching Lin¹ and Ying-Chih Hsu¹

Abstract: This paper uses quasi-steady molecular statics method to carry out simulation of nanoscale orthogonal cutting of single-crystal copper workpiece by the diamond tools with different edge shapes. Based on the simulation results, this paper analyzes the cutting force, equivalent stress and strain, and temperature field. For the three-dimensional quasi-steady molecular statics nanocutting model used by this paper, when the cutting tool moves on a workpiece, displacement of atoms is caused due to the effects of potential on each other. After a small distance that each atom moves is directly solved by the calculated trajectory of each atom, the concept of force balance is used. And Hooke-Jeeves direct search method is also used to solve the force balance equation, and obtain the new movement position. When chip formation and the size of cutting force during cutting are calculated, further analysis is made. After the position of an atom's deformation displacement is acquired, the shape function concept of finite element is employed to obtain the atomic-level equivalent strain. With the stress-strain curve obtained from experiment of the numerical tensile value of nanoscale copper film taken as the foundation, regression treatment is made, and then the flow stress-strain relational equation is acquired. The flow stress-strain curve is used to calculate the equivalent stress produced under equivalent strain of element. This paper further supposes that workpiece temperature is mainly produced from two heat sources: plastic deformation heat and friction heat. Thus, this paper uses the acquired equivalent stress and strain to calculate plastic deformation heat. Besides, this paper additionally develops a method to calculate the numerical value of friction heat produced by the workpiece atoms on the tool face and the numerical value of temperature rise of workpiece atoms on tool face. Finally, the temperature rise produced from the two heat sources is added up for calculation of temperature field of the cut single-crystal copper workpiece during nanoscale orthogonal cutting, and for making analysis.

¹ Department of Mechanical Engineering, National Taiwan University of Science and Technology, Taipei, Taiwan.

Keywords: Quasi-steady molecular statics, Nanoscale orthogonal cutting, Single crystal copper, Temperature.

1 Introduction

To understand nanotechnology properties and forming, analysis can be made through experiments and theoretical simulation. However, experiments usually need expensive equipment, and the subsequent analysis is more difficult, making theoretical analysis more attractive. Molecular dynamics is employed for nanoscale analysis, and molecular dynamics simulation is extensively applied to the studies of nanocutting, nanoindentation, nano tension, etc. With the rapid development of computer technologies, computation speed is being greatly accelerated, further enhancing the development and significance of molecular dynamics simulation in nanoscale studies.

Shimada (1990) used 2D models and molecular dynamics (MD) for the dynamic simulation of orthogonal cutting, and investigated its relation to chip formation. Childs and Maekawa (1990), Belak and Stower (1990) employed molecular dynamics theory for numerical simulation of the orthogonal cutting of copper substrates using a rigid cutting tool, though their model lacked complete quantitative calculation. Kim and Moon (1995) used molecular dynamics to construct a 2D cutting model of a single-crystal diamond cutter for cutting (111) copper material with the highest density plane with [110] cutting direction. That study found that an arc-shaped cutter could produce thinner chip than a sharp cutter. Fang et al. (2007) indicated that the nanoscale cutting action was mainly produced by extrusion, in contrast to the traditional cutting action, where the workpiece is deformed by shearing. Pei et al. (2006) used MD to simulation and study the nanoscale cutting of copper, and pointed out that the rake angle of cutter has significant influence to chip formation and the surface of workpiece. As the rake angle changes from -45° to 45° , both the cutting forces and the ratio of normal cutting force to tangential cutting force (F_y/F_x) decrease considerably. They also found that under the Morse potential results in about 5-70% higher cutting forces than under the embedded atom method (EAM) potential. Inamura et al. (1991,1992) considered atoms as nodes, and used the Morse potential between atoms to deduce the finite element formulation of an atomic model. They took the Morse potentials of two different atoms as examples for simulation, and achieved the chip formation process, and the changing process of cutting force and potential energy along with movement of the cutting tool. With the two-dimensional MD model, Ikawa et al. (1991) investigated the effect of tool edge radius and depth of cut on the chip formation process. Lin and Huang (2004) improved the finite element model developed by Inamura et al. (1993). They used the Morse potential between the cutter and the atoms of

workpiece, and used molecular dynamics, to get the atomic movement to describe the overall cutting process. In their model, atoms were considered as nodes, and lattices as elements. The developed program of their nanoscale orthogonal cutting model was used to calculate the displacement of each atom on the cross-section of the workpiece being cut. Furthermore, they used the concept of shape function in finite element formulation, and the calculated molecular displacement was employed to calculate the material strain. Finally, after the stress-strain curve of the nanoscale film tensile numerical experiment had been through the regression treatment, the acquired flow stress-strain relationship equation was used to calculate the equivalent stress. M. Rahman et al. (2007) applied the MD method to simulate nanoscale ductile mode cutting of monocrystalline silicon. The temperature and mechanics characteristics in the workpiece have been investigated.

With molecular dynamics (MD), its basic principle is the establishment of a particle system to simulate the microscopic phenomenon to be studied. The particle movement follows Newton's law of motion and when quantum effect and multi-body interaction are neglected, the interaction between particles satisfies the superposition principles. Using the dynamics equations of particles, the trajectory of different particles in phase space can be determined by molecular dynamics. Furthermore, the relative properties of the system can be acquired. Nevertheless, the time step for molecular dynamics is too small, thus creating the problems that the simulation process has to spend much time for the calculations, which are difficult.

Therefore, some researchers have used molecular statics to simulate nanoscale studies in order to rectify the problems encountered with molecular dynamics. Kwon et al. (2004) investigated material properties by using atomic model to simulate the equilibrium of static load. They proposed a model that combines the atoms with finite element formulation to simulate the nanoscale tensile problem for the defective material. Telitchev and Vinogradov (2006) used quasi-static analysis to investigate the tensile problem of non-perfect lattice structure. Their paper mentioned that two different methods for solving the static equilibrium position, both used the minimum energy method and allowed the force to reach a relatively small value when atoms were moved. Each equilibrium state of the crystal was described by a linear algebraic equation. This equation had displacement interdependence, so the Inverse Broyden's Algorithm (IBA) was used to solve the atomic trajectory displacement of the system. Jeng and Tan (2004) adopted the combination of molecular statics method with the least energy principle in the finite element as the structure to simulate the displacement and deformation process of nanoindentation. The least potential energy method was primarily used, followed by the displacement control superposition method in the non-linear finite element formulation to solve the relationship between each atomic force and position.

Taking the concept of molecular statics, this paper focuses on single-crystal copper material to carry out nanoscale orthogonal cutting. For the simulation of cutting act, the Morse force of each atom in X, Y and Z directions during cutting is divided to establish force balance equations. This paper also uses engineering optimization method to calculate the optimal displaced position of force balance, and confirms that this new position reaches the minimum energy position of the entire system. Therefore, the new position after force balance is just the minimum energy position. The number of times in calculation of time can be decreased, and the action force produced during cutting of workpiece material by diamond tool can be acquired. In order to prove whether the horizontal cutting force and thrust force obtained from this paper's molecular statics cutting model are reasonable or not, this paper compares the ratio of thrust force to cutting force (F_t/F_c) with the numerical value acquired by Pei et al. (2006). Eventually, the numerical value of cutting force obtained by this paper is proved to be reasonable. Furthermore, it can be derived that the quasi-steady molecular statics nanocutting model of this paper should be reasonable. This paper further applies cutting behavior model, together with analysis of equivalent stress and equivalent strain, to observe the distribution trend of equivalent strain and equivalent stress after cutting, making the exploration of the entire nanocutting simulation becomes more complete.

During nanocutting simulation, the materials to be cut are mostly supposed to be of perfect crystal structure. This paper employs the concept of molecular statics to carry out orthogonal cutting of 3D perfect-crystal copper material, and calculate the cutting force, equivalent stress and strain, and heat source temperature. Currently, molecular dynamics model was commonly used in the past literature to simulate heat source temperature. This paper develops the method of using molecular statics to carry out cutting simulation, and then uses the Morse force and equivalent strain acquired from simulation to calculate friction heat source temperature and plastic deformation heat source temperature, and find the temperature field. Furthermore, this paper analyzes the physical phenomenon in times of machining, and explores whether the change of cutting parameters would cause the production of cutting force and temperature heat source of material and create effects. Using round-edge tool and cutting depth 1.08nm, and through simulation of molecular statics orthogonal cutting, this paper calculates the temperature rise of copper workpiece and temperature field distribution. In addition, this paper makes qualitative validation and comparison with the temperature distribution result of a nanocut copper workpiece in a fluid-free (vacuum) environment as obtained from simulation made by Rentsch and Inasali (2006) with the use of molecular dynamics, and analyzes its physical phenomenon.

2 The three dimensional quasi-steady molecular statics nanocutting model

2.1 Calculation of cutting force

The quasi-steady molecular statics nanocutting model of this paper uses the adopts Morse potential energy of two-body potential energy as the basis for calculation of the action force between molecules. The equation of Morse potential energy [Girifalco and Weizer (1959)] is expressed as follows:

$$\Phi(r_{ij}) = D \left\{ e^{-2\alpha(r_{ij}-r_0)} - 2e^{-\alpha(r_{ij}-r_0)} \right\} \quad (1)$$

D : binding energy

α : material parameter

r_{ij} : distance between two atoms

r_0 : equilibrium distance

This paper adopts Morse's two-body potential energy function to describe the interaction force between molecules when the diamond cutter is cutting a copper workpiece. The Morse potential energy function parameters used between the carbon atoms of diamond cutter and the copper atoms of the workpiece is shown in Table 1 [Zhang and Tanaka(1997)].

Table 1: Morse potential energy function parameters between diamond cutter and atoms of copper workpiece material.

	Cu-Cu	Cu-C
D : binding energy (eV)	0.3429	0.087
α : material parameter (\AA)	1.3588	5.140
r_0 : equilibrium distance between atoms (\AA)	2.8660	2.050

For the general potential energy function, when the distance between two atoms is greater than a certain distance, the action force between atoms will decrease rapidly. Therefore, we define the distance cut-off radius r_c , and when the distance exceeds r_c , the action force is very small so it does not need to be calculated. In this way, the calculation can be tremendously simplified. Therefore, the Morse potential energy of the distance between two atoms inside r_c and outside r_c can be further expressed as equation (2):

$$\begin{cases} \Phi(r_{ij}) = D \left\{ e^{-2\alpha(r_{ij}-r_0)} - 2e^{-\alpha(r_{ij}-r_0)} \right\} & r \leq r_c \\ \Phi(r_{ij}) \cong 0 & r \geq r_c \end{cases} \quad (2)$$

According to the Morse potential used by this paper, the action force between two atoms can be expressed as equation (3):

$$F(r_{ij}) = -\frac{\partial\Phi(r_{ij})}{\partial(r_{ij})} = 2D\alpha \left\{ e^{-2\alpha(r_{ij}-r_0)} - 2e^{-\alpha(r_{ij}-r_0)} \right\} \quad (3)$$

When $r_{ij}=r_0$, the action force between atoms is just situated at a balance between attraction force and repulsive force. Both the cutter and workpiece material are at the situation of no action force. When $r_{ij}<r_c$, the diamond cutter and copper material will produce action force. As known from equation (3), when r_{ij} value is smaller, the action force produced between two atoms will be greater, making the copper material of workpiece pushed away from the original balanced position by the action force. As the step of cutter moves forward, the so-called chip phenomenon is formed.

By using equation (3), we can infer that the action force between two atoms can be expressed as equation (4):

$$\vec{F}_i = \sum_{i=1}^n \vec{F}_{ij}(r_{ij}) \quad (4)$$

i : a number given to the carbon atom of cutter.

j : a number given to the copper atom in material.

n : number of copper atoms.

r_{ij} : distance between two atoms.

The action force between two atoms acquired from equation (3) can be further divided into the components of force in two axes, \vec{F}_x , \vec{F}_y and \vec{F}_z , as shown in equation (5):

$$\vec{F}_i = \vec{F}_{x_i} + \vec{F}_{y_i} + \vec{F}_{z_i} \quad (5)$$

\vec{F}_{x_i} : component of force of the action force in X direction

\vec{F}_{y_i} : component of force of the action force in Y direction

\vec{F}_{z_i} : component of force of the action force in Z direction

Of course, after cutting has proceeded for a certain period, there is not just one copper workpiece atom influenced by the Morse force of the diamond cutter. Hence, the Morse force vector of each copper atom of the copper workpiece being affected by the Morse force of diamond cutter after having moved to the new position, as well as the Morse force of other copper atoms inside the cut-off radius acted on by each atom after moving to the new position are used in sequential order to find the

sum of Morse force vector of each copper atom. The sum of Morse force vector are further resolved as the Morse force component F_X in the X direction as well as the Morse force component F_Y in Y direction and F_Z in Z direction. As mentioned above, let the sum of the Morse force components in the X, Y and the Z directions be zero respectively. Then the force equilibrium equation of the quasi-steady molecular statics nanocutting model is formed, as shown in equation (6).

$$F_X = \sum_{i=1}^m \vec{F}_{ix}(r_{ij}) = \sum_{i=1}^m \sum_{j=1}^n F_x(r_{ij}) = 0 \quad (6)$$

$$F_Y = \sum_{i=1}^m \vec{F}_{iy}(r_{ij}) = \sum_{i=1}^m \sum_{j=1}^n F_y(r_{ij}) = 0$$

$$F_Z = \sum_{i=1}^m \vec{F}_{iz}(r_{ij}) = \sum_{i=1}^m \sum_{j=1}^n F_z(r_{ij}) = 0$$

i : numbers assigned to all the atoms of diamond cutters that affect the Morse force of a certain copper atom.

j : numbers assigned to other copper atoms inside the cut-off radius other than a certain copper atom affected by the Morse force of cutter.

m : quantity of all the diamond cutter atoms when corresponding to a certain copper atom affected by the Morse force of cutter.

n : quantity of other copper atoms inside the cut-off radius other than a certain copper atom affected by the Morse force of cutter.

r_{ij} : distance between the j th copper atom in the copper material and the corresponding i th atom of diamond cutter, and the distance between the j th copper atom and the corresponding i th copper atom.

It is really not easy to solve the differential expressions of this paper's component F_X in X direction, component F_Y in Y direction and component F_Z in Z direction, thus making it difficult to construct the related programs. Hence, this paper proposes the use of optimization concept to find the most suitable displacement position. To find the most suitable displacement position by optimization search method, we firstly have to define a searching range. Since the feeding of each step does not exceed 0.002\AA in this paper and it is not easy for the atom to go through another atom to conduct deformation, this paper supposes that each feeding does not exceed the distance of 1/2 lattice constant, so as to search the most suitable force balance deformation and displacement position for the feeding of each step.

Hooke-Jeeves search method is employed to carry out the search. First of all, the starting point has to be defined. In each cutting step, the copper atom affected by the Morse force of the diamond cutter is the starting point of search. The increment of search is 0.001\AA , and the convergence value $\varepsilon=10^{-4}$. The above logic is used to carry out the search of the most suitable displacement position point in each step, which is just our acceptable new point of force balanced displacement position.

Focusing on the nanoscale orthogonal cutting simulation of perfect crystalline-lattice single-crystal copper, this paper proposes the following methods. First of all, the new coordinates of atoms after displacement in each step are calculated. Then, the atoms are numbered. According to finite element method (FEM), segmented grids are arrayed and numbered one by one. Based on these numbers, they are substituted in cut-off radius equation, Morse potential function, force balance as well as stress and strain equations in proper order. The calculated equivalent strain and Morse force are respectively substituted in the equations for calculation of plastic heat source and friction heat source. Adding these two heat sources up, the temperature field distribution of workpiece can be found.

2.2 Calculation of equivalent stress and equivalent strain

After the new position of each copper atom for the feed of diamond tool in each step is calculated, this paper compares the new position of each atom with its original position, acquiring the displacement of each copper atom. The relationship between displacement function and node in FEM is further applied, with the various copper atoms regarded as nodes. Furthermore, the equivalent strain of copper atom element is calculated. After that, the equivalent strain-stress curve equation acquired by Rau (1999) after simulation of the numerical tensile value of nanoscale copper film is used to further calculate the numerical value of equivalent stress of copper atom element during this time.

After using the abovementioned quasi-steady molecular statics nanocutting model to acquire the feed of diamond tool in each step, as well as the newly displaced position of each copper atom of the cut copper workpiece, and before analyzing equivalent strain and equivalent stress, there has to be a fracture criterion of element for making judgment. When a diamond tool enters a workpiece, cutting force makes the atoms of workpiece displaced, leading to deformation of the copper lattice element composed of copper atoms of workpiece. When deformation of the copper lattice element is greater than a certain extent, lift-off phenomenon is caused between element and element, and chips are formed. Thus, there has to be a fracture criterion of elements to make the calculated numerical values of equivalent strain and equivalent stress become reasonable.

According to the chip lift-off criterion of Lin and Huang (2004) that combines

Morse potential with the space limitation rule of a rigid cutter, there are two conditions mentioned. When one of the two conditions is met during cutting, the element can be regarded as being fractured, as shown as Fig. 1. The conditions of these two lift-off criteria are described as follows:

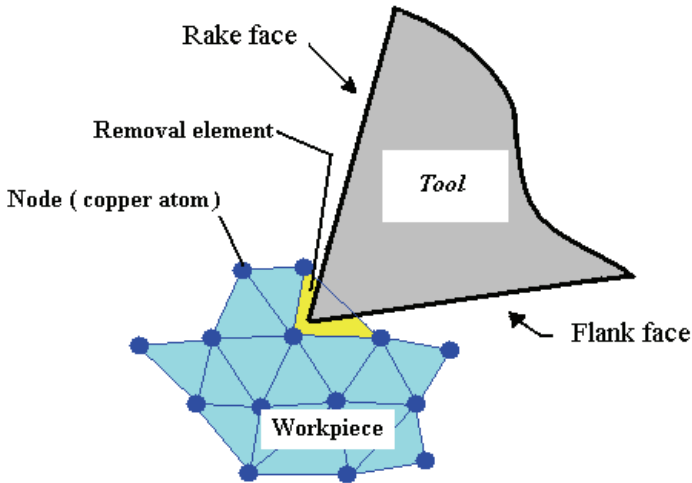


Figure 1: Schematic illustration of the chip lift-off criterion of the cutting of diamond cutter.

When any two nodes of a certain triangular element are located at the rake face and clearance face of a diamond rigid cutter respectively, it implies that the elements of these two nodes are fractured for being cut by the diamond cutter. Thus, this triangular element should be removed.

When the distance between any two nodes of a triangular element is greater than the distance that both can attract each other, it implies there is no interrelation between these two nodes. The distance available for mutual attraction is defined as the distance that is greater the length of 2.5 times the equilibrium distance (r_0) of copper atoms plus 1 Å. Therefore, if the distance between any two nodes of a certain triangular element is greater than the defined distance available for mutual attraction, it indicates that this element is fractured. Thus, this element will be removed.

Since the orthogonal cutting is used in this study, the error of position change of the atoms on each cross-section near the central part of material is small, so that this paper only takes the positions of atoms on the cross-section near the center of the cut workpiece. As shown in Fig. 2, under the condition that plane strain is

considered, two-dimensional way is used to calculate equivalent strain and equivalent stress. Employing the calculation model of Lin and Huang (2004), this paper calculate the equivalent stress-strain relationship, and proposes that for the displacement of copper atoms, the relational equation between strain of continuum mechanics and displacement can be used to acquire atomic-level equivalent strain. This is because strain-displacement relationship is purely a transformation of geometric relationship, instead of a relationship of mechanics, so that there should be no doubt caused. Therefore, after using molecular statics to calculate the newly displaced position of the atom in each step, strain-displacement relational equation can be used to obtain the atomic-level equivalent strain.

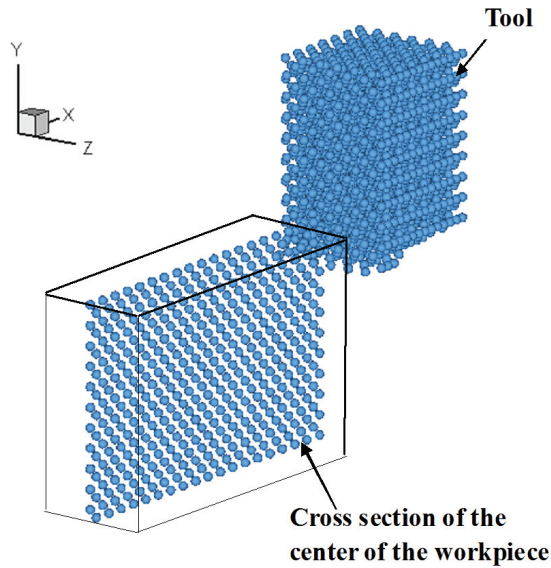


Figure 2: Schematic diagram of the analyzed cross-section

Thus, the strain-displacement relationship equation is deduced as follows:

$$\{\varepsilon\} = \begin{Bmatrix} \varepsilon_x \\ \varepsilon_y \\ \varepsilon_{xy} \end{Bmatrix} = \frac{1}{2A} \begin{Bmatrix} \beta_i & 0 & \beta_j & 0 & \beta_m & 0 \\ 0 & \gamma_i & 0 & \gamma_j & 0 & \gamma_m \\ \gamma_i & \beta_i & \gamma_j & \beta_j & \gamma_m & \beta_m \end{Bmatrix} \begin{Bmatrix} u_i \\ v_i \\ u_j \\ v_j \\ u_m \\ v_m \end{Bmatrix} = \{B\} \{\delta\} \quad (7)$$

where $\{\varepsilon\}$ is the strain matrix of element, $\{B\}$ is the displacement-strain relation-

ship matrix and $\{\delta\}$ is the node displacement matrix.

It can be seen that that after the displacement component of copper atoms has been acquired from the quasi-steady nano-cutting model, the strain of the triangular element can be obtained from equation (7). Then, from the acquired strain of element made up of copper atoms in the equation, the equivalent strain can be further calculated.

Regarding the equation for the relationship curve between equivalent strain and equivalent stress, this paper uses equation (8) of the equivalent stress-equivalent strain curve acquired from Rau's (1999) simulation experiment of the numerical tensile value of nanoscale copper film, as the basis. Then, the relationship curve between equivalent stress and equivalent strain required by the paper can be acquired. According to equation (8) and the equivalent strain calculated above, the equivalent stress produced under the equivalent strain of each element can be calculated.

$$\begin{aligned}\bar{\sigma} &= 1.9621 + 3.2966\bar{\varepsilon}, 0 \leq \varepsilon \leq 0.3 \\ \bar{\sigma} &= 3.69293\bar{\varepsilon}^{0.1817}, \varepsilon > 0.3\end{aligned}\quad (8)$$

2.3 Calculation of temperature rise of the cut workpiece during nanocutting

This paper carries out quasi-steady molecular statics simulation in three-dimensional way, and the initial temperatures of workpiece and cutting tool are both supposed to be at room temperature (300K). However, the cutting state is orthogonal cutting, and is in symmetric shape in Z direction of the workpiece width. Thus, the heat transfer effect on the Z axis can be neglected, and exploration can only be made for the temperature distribution on the cross-section near the center in X and Y directions.

In the nanocutting machining process, this paper supposes that the main heat is produced from two heat sources as follows:

1. Plastic deformation heat produced from quasi-plastic deformation, which is caused by deformation between atoms of workpiece.
2. Friction heat produced between workpiece atoms and tool atoms.

This paper applies the equivalent stress calculated by the three-dimensional quasi-steady molecular statics nanocutting simulation model developed by this paper, and then substitutes it in the flow-stress curve to obtain equivalent strain. Multiplying the equivalent stress by the equivalent strain, the heat produced by the plastic heat source of quasi-plastic deformation can be acquired. Besides, applying the calculation method of nanocutting force with the use of quasi-steady molecular statics nanocutting model, this paper can acquire the force balance of Morse force and

the instant displacement increment of workpiece atoms. With the concept of force balance, the total Morse force borne by the copper workpiece atoms in contact with the tool face can be decomposed to be component force in X, Y and Z directions. Furthermore, the Morse force borne by each workpiece atom being close to the tool face is decomposed to be normal component force and tangential component force on the tool face. The component force in tangential direction is just the force similar to friction force produced by cutting of workpiece. The product of multiplying the friction force borne by atoms by the displacement of atoms along the tangential side of cutting tool can be regarded as the friction heat produced by the quasi-friction of workpiece atoms on the tool face.

Currently, towards solving the problems of nanocutting, most researchers commonly use three-dimensional molecular dynamics to solve the cutting temperature field. To solve the chips and temperature distribution inside the workpiece, there is still no one using the concept of combining quasi-steady molecular statics nanocutting simulation model with the heat source mentioned above in this paper.

This paper supposes that in the workpiece atoms in contact with the tool face, friction heat is produced in the various atoms with the adjacent distance between the workpiece atoms bearing Morse force and the tool atoms being smaller than 1 Å. Therefore, Δd_{fi} is supposed to be the displacement increment of workpiece atoms on the tool face in tangential direction. Thus, $\Delta d_{fi} = v_{fi}\Delta t$.

As mentioned above, friction heat is supposed to be produced from the friction between the atoms on cutting tool and the workpiece atoms. The calculation method is shown as follows:

$$Q_{fi} = \frac{F_{fi}v_{fi}\Delta t}{J} \quad (9)$$

where F_{fi} : friction force on the tool face after decomposing the Morse force borne by workpiece atoms.

v_{fi} : tangential speed of the interface between workpiece atoms and the tool face atoms.

Δt : time interval.

For the product of multiplying the equivalent stress by equivalent strain of each element obtained in the nanocutting simulation model, this paper regards it as quasi-plastic heat source. Therefore, within the time Δt of workpiece, this paper supposes that the temperature rise caused by quasi-plastic deformation is:

$$\Delta T_d = \frac{\int \bar{\sigma} \bar{\epsilon} \Delta t}{Jc\rho} \quad (10)$$

where c is the specific heat, and ρ is the density of material.

Since the abovementioned friction heat is produced on the various workpiece atoms contacting along the tool face direction, they are distributed to the nearest cutting tool and workpiece atoms in α_w/α_t proportion. Thus, the temperature rise distributed to the workpiece and the tool face are ΔT_{wi} and ΔT_{ti} respectively, being equation (11) as follows (Lin et al., 1995):

$$\Delta T_{wi} = \frac{\alpha_w}{\alpha_w + \alpha_t} \frac{1}{c_w \rho_w v_w} Q_{fi}$$

$$\Delta T_{ti} = \frac{\alpha_t}{\alpha_w + \alpha_t} \frac{1}{c_t \rho_t v_t} Q_{fi} \quad (11)$$

where $\alpha_w = \left(\frac{k_w}{c_w \rho_w} \right)^{\frac{1}{2}}$, $\alpha_t = \left(\frac{k_t}{c_t \rho_t} \right)^{\frac{1}{2}}$.

In the equation, v_w and v_t are the volume of particles on the interface of workpiece and cutting tool respectively, whereas k_w and k_t are the thermal conductivity coefficients of workpiece and cutting tool respectively.

3 Construction of simulation model

This paper uses the constructed quasi-steady molecular statics cutting model to simulate cutting of copper workpiece by a diamond tool. The simulation is undertaken in three-dimensional way. This paper carries out simulation of nanoscale orthogonal cutting by the cutting tools with four different edge shapes. The first, third and fourth cutting tools are the round-edge diamond tools, all with clearance angle 10° and edge radius 5\AA at their front tips, but with rake angles being 0° , 15° and -15° respectively. The second cutting tool is a sharp diamond tool with clearance angle 10° and rake angle 0° . The construction of the cutting tool and the workpiece material to be cut are shown in Fig. 3. Table 2 shows the parameters for calculation during simulation.

For the cutting of metal, the copper material to be cut is relatively softer than diamond tool. Therefore, the paper regards diamond tool as a rigid body. Besides, when the distance between two atoms reaches 5\AA , Morse potential function is almost zero. Hence, the cut-off radius is supposed to be 5\AA .

During simulation, comparison is made for the orthogonal cutting of a perfect crystalline lattice material by different cutting tools. Taking the four simulation examples, analyses are further made. Figure 4 shows the initial simulation diagram of the relative positions of the tool and the workpiece.

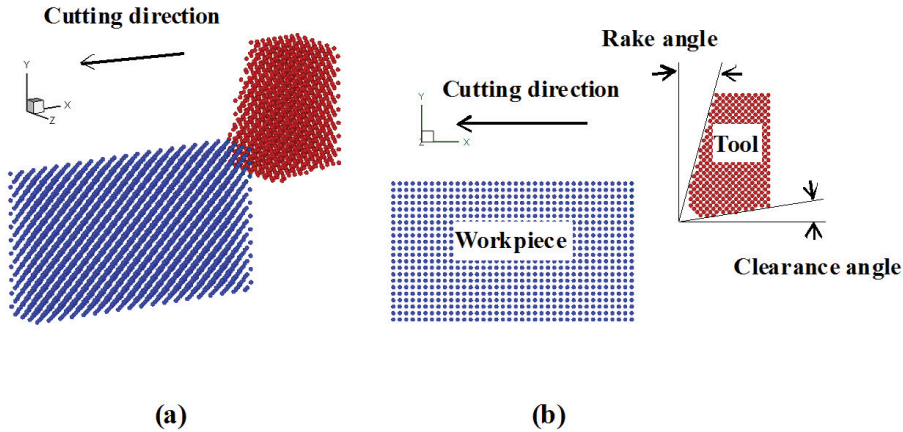


Figure 3: 3D quasi-steady molecular statics nanoscale orthogonal cutting model. (a) 3D image, (b) Side view.

Table 2: Computational parameters used in the 3D quasi-steady molecular statics simulation of nanoscale cutting of a copper workpiece.

Configuration	Nanocutting			
Copper (workpiece material)	6a x 5a x 5a, where a is the lattice constant of copper (3.61Å), atoms: 3344			
Tool edge radius (nm)	0.5	0	0.5	0.5
Rake angle	0°	0°	15°	-15°
Clearance angle	10°			
Depth of cutting (nm)	1			
Width of cutting (nm)	1.81			

4 Results and discussion

4.1 Validation and comparison of simulation

4.1.1 Validation and comparison of cutting forces after cutting simulation of single-crystal material

In order to prove that the cutting forces simulation used in this paper are feasible, this paper lets a group of nanocutting simulation parameters be identical to the nanocutting simulation parameters indicated in the paper of Pei et al. (2006). This paper carries out orthogonal cutting simulation by letting a sharp diamond tool,

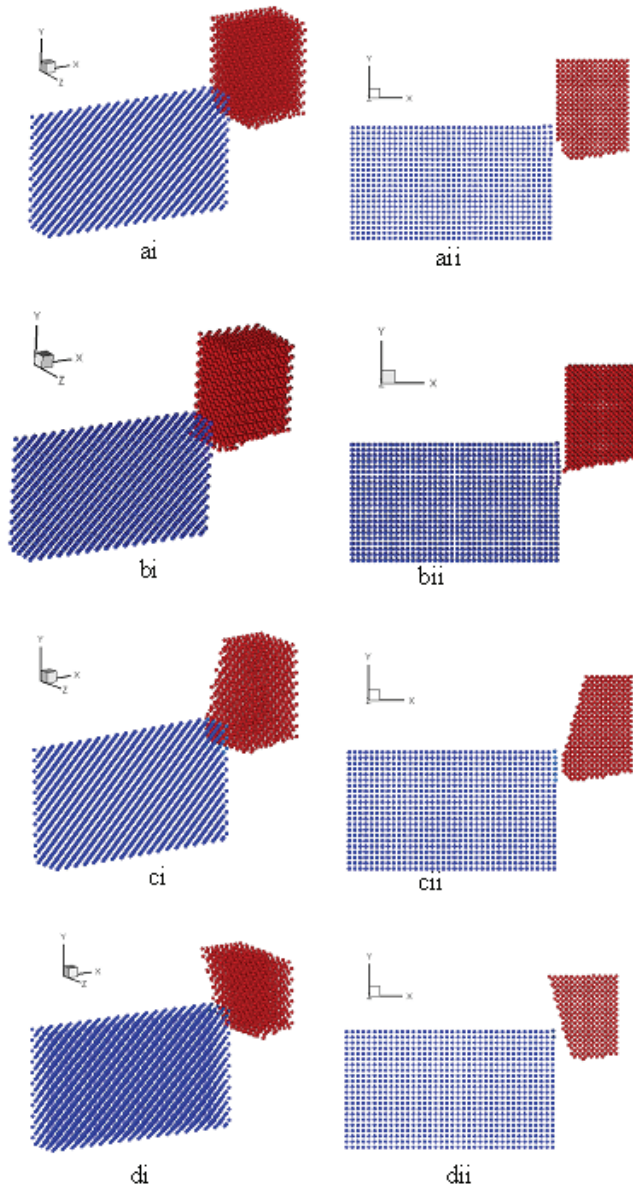


Figure 4: Diagrams of initial conditions of different simulation examples. (a) the round-edge diamond cutter with nose radius of 5\AA , rake angle of 0° . (b) the sharp diamond cutter with rake angle of 0° (c) the round-edge diamond cutter with nose radius of 5\AA , rake angle of 15° . (d) the round-edge diamond cutter with nose radius of 5\AA , rake angle of -15° and the perfect lattice copper workpiece material.

with its rake angle set to be 0° and clearance angle 10° , cut the depth of 1.08nm on a single-crystal copper workpiece at the width 18.1Å (width of 5 lattices). The numerical value of cutting force resulted from simulation is compared with the numerical value of cutting force acquired in the paper of Pei et al. (2006). The initial coordinates of the tool tip are set to be at the position with a horizontal distance 5.0 Å on the right hand side of the workpiece. The cutting tool moves towards the workpiece at the feed 0.002 Å per step, and simulates the cutting of the workpiece at the width of 5 copper lattices. After analysis on simulation of cutting force and thrust force from the three-dimension quasi-steady molecular statics nanocutting simulation equation developed by this paper, it is found that after the 12,000th step, the cutting force starts to be steady. Therefore, the paper lets the average numerical value of cutting force after the 14,000th step be 37.8nN, the average numerical value of thrust force be 24.6nN, the ratio of thrust force to cutting force (F_t/F_c) be 0.65, which is further compared with the numerical value of F_t/F_c 0.64 obtained from the simulation of Morse potential undergone by Pei et al. (2006). Related comparison results are shown in Table 3. From Table 3, it can be seen that both simulation results are quite similar. Thus, it is proved that the nanoscale orthogonal cutting simulation equation developed by this paper is acceptable.

Table 3: Comparison of the results of cutting force and thrust force between simulation of cutting workpiece at the width of 5 lattices undergone by the paper and simulation of reference [Pei et al. (2006)].

	Cutting force F_c (nN)	Thrust force F_t (nN)	F_t/F_c
Sharp diamond cutter and the rake angle is 0°	37.8	24.6	0.65
Pei 's numerical value	39	25	0.64

4.1.2 Validation and comparison of temperature distribution of the cut workpiece after simulation of cutting of perfect crystalline-lattice single-crystal copper material

In order to prove the feasibility of applying the quasi-steady molecular statics nanocutting model developed by this paper and further applying the abovementioned theoretical model for calculation of the temperature rise caused by plastic heat source and friction heat source of the cut workpiece, this paper carries out simulation of cutting by letting a round-edge diamond tool, with its rake angle set to be 0° and edge radius 5Å at its tip, cut the depth of 1.08nm on a single-crystal copper workpiece at the width 18.1Å (width of 5 lattices). Then, qualitative comparison

is made between the simulation result of numerical temperature value and the cutting temperature distribution in vacuum state as indicated in the paper of Rentsch and Inasaki (2006), who used molecular dynamics for simulation and calculated the cutting temperature distribution of the cut single-crystal copper workpiece. As seen from this paper's simulation result of cutting temperature of the cut single-crystal workpiece, after the 12,000th step the cutting force tends to be steady. Therefore, we take the numerical temperature value of the 14,000th step and the temperature distribution diagram, achieving the results that the highest temperature of atoms on the single-crystal copper chips is around 783K, and the highest temperature of a single-crystal copper workpiece close to the tip zone is between 750 and 783K. But in the paper of Rentsch and Inasaki (2006), the workpiece temperature in the tip zone is around 750K. Since the temperature calculated by Rentsch and Inasaki (2006) is the zone temperature, and the data of the zone temperature calculated by this paper is close to that of the reference, their rough numerical values of temperature distribution and their qualitiveness are close and acceptable.

The slight distance between the value acquired by this paper and the data acquired by Rentsch and Inasaki (2006) is possibly because of the greater edge radius of the cutting tool used by Rentsch and Inasaki (2006), and the different calculation methods of temperature between the use of molecular dynamics cutting simulation model by Rentsch and Inasaki (2006) and the use of quasi-steady molecular statics nanocutting simulation model by this paper. For the calculation method of cutting temperature using molecular dynamics, the kinetic energy of atoms with high-speed movement is converted into heat source. But for the paper's calculation method of cutting temperature using molecular statics, it calculates the temperatures of two heat sources, including the plastic deformation heat of atoms and the friction heat on the tool face. Therefore, the result calculated by this paper is different from the numerical value of cutting temperature calculated by Rentsch and Inasaki (2006). But their results of temperature distribution and qualitiveness are still very similar. Therefore, the nanoscale orthogonal cutting simulation developed by this paper is proved to be acceptable.

4.2 Exploration of the cutting of a single-crystal copper workpiece by cutting tools with different edge shapes

As mentioned above, the cutting tools used by this paper include a sharp diamond tool with rear angle 0° and clearance angle 10°, and three round-edge tools with rake angles being 0°, 15° and -15° respectively, and all with clearance angle 10° and edge radius 5Å at their tips. Let the coordinate of cutting tool in X direction be at a distance 5.0Å from the copper workpiece, and let the feed of each step each time be the cutting feed 0.002Å, for undergoing the nanocutting simulation

act of copper material at the width of 5 lattices, and for analyzing the distribution of cutting temperature.

4.2.1 Investigation of cutting force

During exploration of cutting force, the mutual attraction force between diamond tool and single-crystal copper workpiece in times of cutting is defined as a negative value, whereas the repulsive force is set to be a positive value. Figure 5 shows the diagram of numerical values of the orthogonal cutting force, thrust force and side force acquired from simulation of orthogonal cutting of a single-crystal copper workpiece by a round-edge tool with rake angle 0° , clearance angle 10° and edge radius 5\AA . As found in Fig.5, whenever the cutting tool moves forward for one step, the cutting force is slightly vibrated, and the peak value becomes greater and greater until the cutting tool cuts in the workpiece for a distance. By then, a more stable peak value appears. The simulation of this paper is more stable from the $12,000^{\text{th}}$ step to the $18,000^{\text{th}}$ step. Therefore, this paper takes the numerical value in the $14,000^{\text{th}}$ step for analysis of the result. In Fig. 5, the stable numerical value of cutting force is around 41.9nN , the stable numerical value of thrust force is around 27.4nN , and the side force is around 0.4nN .

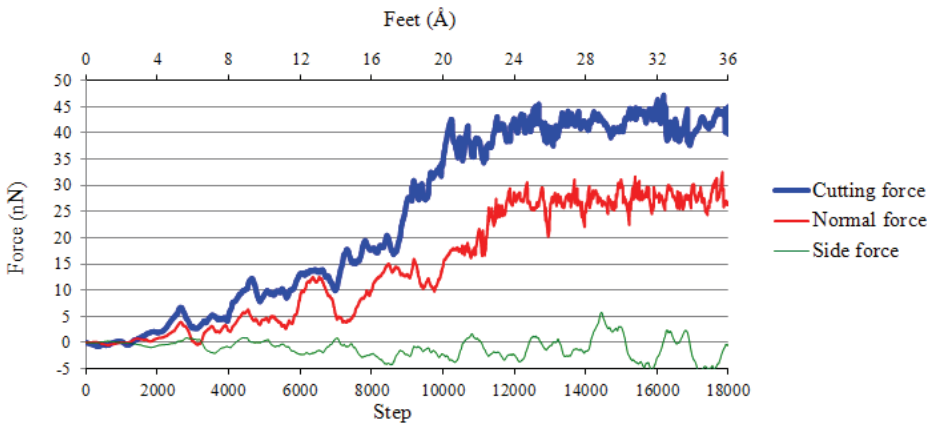


Figure 5: Diagram of cutting force, thrust force and side force acquired from simulation of orthogonal cutting of a single-crystal copper workpiece by a round-edge tool with rake angle 0° and clearance angle 10° .

Figure 6 shows the diagram of the numerical values of cutting force, thrust force and side force acquired from simulation of orthogonal cutting of a perfect-crystal

copper workpiece by a sharp-edge tool with rake angle 0° and clearance angle 10° . In Fig. 6, the stable numerical value of cutting force is around 37.8nN, the stable numerical value of thrust force is around 24.6nN, and the side force is finally also close to 1.04nN. Since the workpiece area in contact with the round edge of tool is greater than that with the sharp tip of tool, the numerical value of cutting force in Fig. 5 is greater than that of sharp tool in Fig. 6.

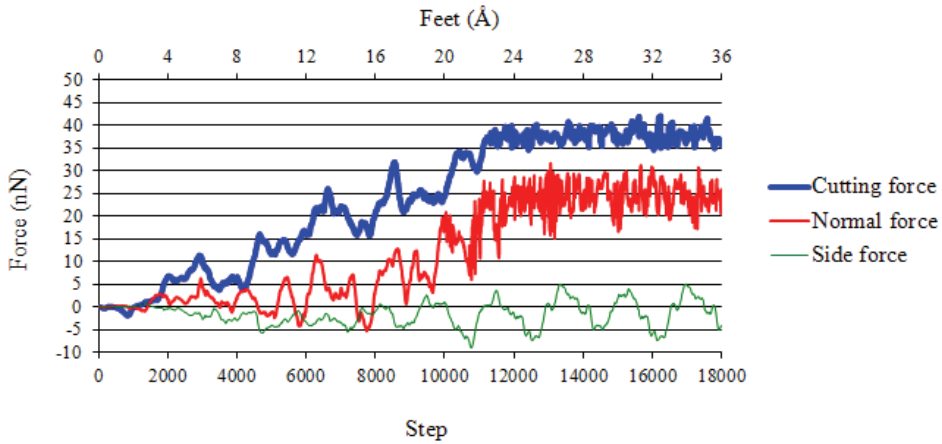


Figure 6: Diagram of numerical values of cutting force, thrust force and side force acquired from simulation of orthogonal cutting of a single-crystal copper workpiece by a sharp-edge tool with rake angle 0° and clearance angle 10° .

Figure 7 shows the diagram of the numerical values of orthogonal cutting force, thrust force and side force acquired from simulation of orthogonal cutting of a perfect-crystal copper workpiece by a round-edge tool with rake angle 15° , clearance angle 10° and edge radius 5\AA . In Fig. 7, the stable numerical value of cutting force is around 36.5nN, the stable numerical value of thrust force is around 23.8nN, and the side force is around 0.94nN. As known from Fig. 7, the cutting force is smaller than that of simulation by a tool with rake angle 0° in Fig. 5. And this phenomenon also occurs to thrust force.

Figure 8 shows the diagram of the numerical values of orthogonal cutting force, thrust force and side force acquired from simulation of orthogonal cutting of a single-crystal copper workpiece by a round-edge tool with rake angle -15° , clearance angle 10° and edge radius 5\AA . In Fig. 8, the stable numerical value of cutting force is around 46.2nN, the stable numerical value of thrust force is around 48.4nN, and the side force is around 5.42nN. Since the workpiece area in contact with the

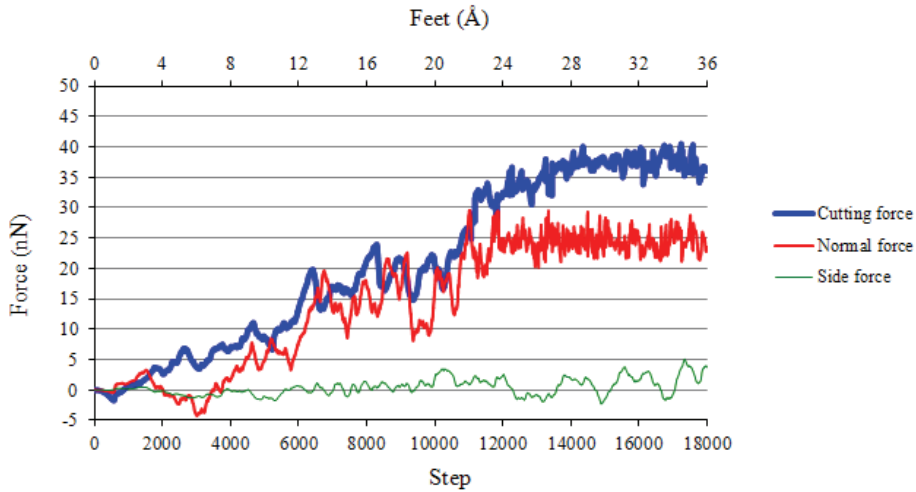


Figure 7: Diagram of numerical values of cutting force, thrust force and side force acquired from simulation of orthogonal cutting of a single-crystal copper workpiece by a round-edge tool with rake angle 15° and clearance angle 10° .

negative rake angle of tool is greater than that with the positive rake angle of tool, the numerical value of cutting force in Fig. 8 is greater than the cutting force simulated by a round-edge cutting tool with rake angle 15° in Fig. 7. And the thrust force is also greater than the cutting force in Fig. 8.

The stable average numerical values of cutting force and thrust force acquired from simulation of orthogonal cutting by four different cutting tools are summarized by the paper in Table 4. From Table 4, it can be seen that the workpiece area in contact with the round edge of tool is greater than that with the sharp edge of tool. Besides, as the rake angle increases towards positive direction, the cutting force is getting lower. And this phenomenon also occurs to thrust force. Besides, it is known that a negative rake angle would increase the contact area between cutting tool and the front end of workpiece chips. This is why when the rake angle moves towards negative direction, the cutting force increases.

4.2.2 Analysis on the numerical values of equivalent strain and equivalent stress in nanocutting condition

Using this paper's calculation method of nanoscale stress and strain mentioned above, the paper calculates the equivalent strain and equivalent stress on the cross-section near the center of a single-crystal copper workpiece after cutting of copper

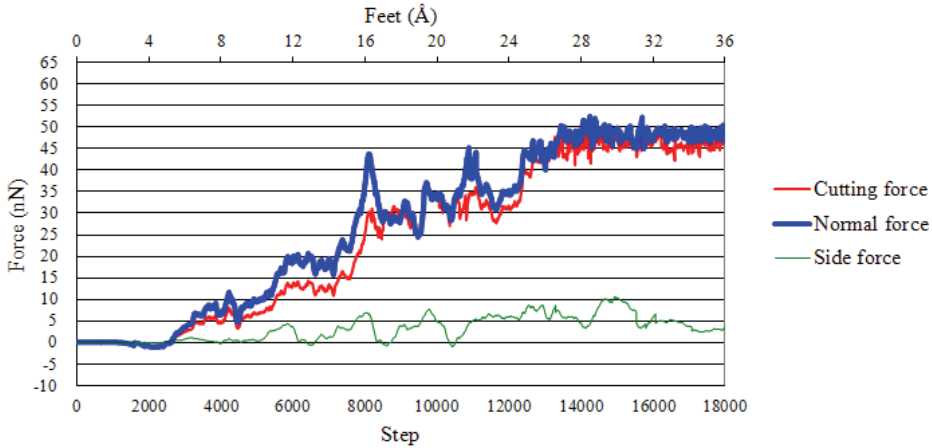


Figure 8: Diagram of numerical values of cutting force, thrust force and side force acquired from simulation of orthogonal cutting of a single-crystal copper workpiece by a round-edge tool with rake angle -15° and clearance angle 10° .

Table 4: Stable average numerical values of cutting force and thrust force acquired from simulation of orthogonal cutting of single-crystal copper material by different diamond tools

	Cutting force (nN)	Thrust force (nN)
Round edge tool with rake angle 0°	41.9	27.4
Sharp edge tool with rake angle 0°	37.8	24.6
Round edge tool with rake angle 15°	36.5	23.8
Round edge tool with rake angle -15°	46.2	48.4

workpiece material. In order to know the distribution of equivalent strain and equivalent stress, the paper draws the diagrams of distribution curves for equivalent strain and equivalent stress on the cross-section near the center of the cut single-crystal copper workpiece, as shown in the figures from Fig. 9 to Fig. 12 respectively.

When this paper take the cutting at the $12,000^{th}$ step to observe the distribution trend of equivalent stress and equivalent strain on the cross-section near the center of a single-crystal copper workpiece, and when the patterns of equivalent stress and equivalent strain are close to the place around the cutting tool, there appears a distribution trend in cluster shape. Figure 9 shows the diagram of equivalent stress and equivalent strain of a perfect-crystal copper workpiece cut by a round edge tool with rake angle 0° , clearance angle 10° and edge radius 5\AA . Based on the numerical

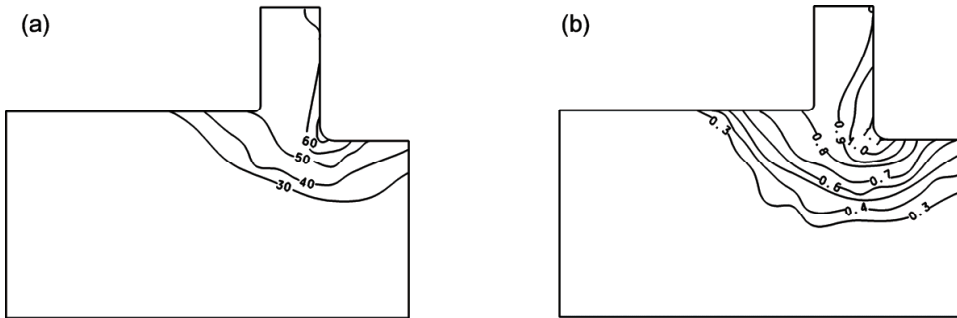


Figure 9: Diagrams of (a) equivalent stress, and (b) equivalent strain, acquired from simulation of orthogonal cutting of a single-crystal copper workpiece by a round edge tool with rake angle 0° and clearance angle 10° .

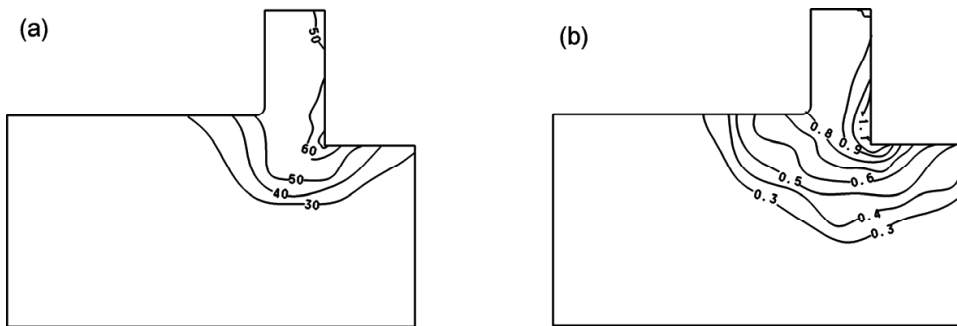


Figure 10: Diagrams of (a) equivalent stress, and (b) equivalent strain, acquired from simulation of orthogonal cutting of a single-crystal copper workpiece by a sharp edge tool with rake angle 0° and clearance angle 10° .

values acquired from our simulation of nanoscale equivalent strain and equivalent stress, it is known that during cutting by a round-edge diamond tool with rake angle 0° , the numerical value of maximum equivalent strain produced is around 1.5, and that of maximum equivalent stress is around 71GPa. Figure 10 shows the diagram of equivalent stress and equivalent strain of a single-crystal copper workpiece cut by a sharp edge tool with rake angle 0° and clearance angle 10° . The numerical value of maximum equivalent strain produced is around 1.3, and that of maximum equivalent stress is around 68GPa. As found in the figures, the numerical values of stress and strain produced on workpiece by a round edge tool are both greater than those by a sharp edge tool. This is possibly because the area of the round edge of tool is greater than the sharp edge of tool, so that the area in contact with the work-

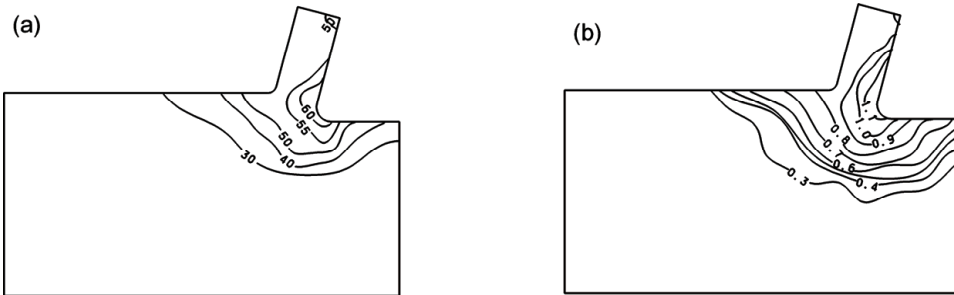


Figure 11: Diagrams of (a) equivalent stress, and (b) equivalent strain, acquired from simulation of orthogonal cutting of a single-crystal copper workpiece by a round edge tool with rake angle 15° and clearance angle 10° .

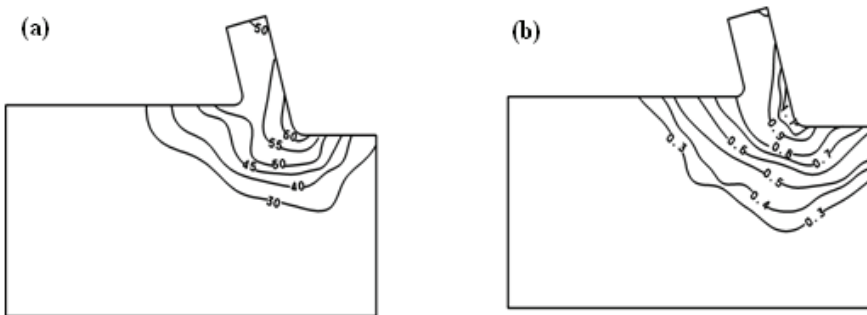


Figure 12: Diagrams of (a) equivalent stress, and (b) equivalent strain, acquired from simulation of orthogonal cutting of a single-crystal copper workpiece by a round edge tool with rake angle -15° and clearance angle 10° .

piece is also greater, and the squeezing layer produced is also wider. This is why greater numerical values are resulted. Figure 11 shows the diagram of equivalent stress and equivalent strain of a perfect-crystal copper workpiece cut by a round edge tool with rake angle 15° , clearance angle 10° and edge radius 5\AA . The numerical value of maximum equivalent strain produced is around 1.2, and the numerical value of maximum equivalent stress produced is around 65GPa. Figure 12 shows the diagram of equivalent stress and equivalent strain of a perfect crystalline lattice copper workpiece cut by a sharp edge tool with rake angle -15° and clearance angle 10° . The numerical value of maximum equivalent strain produced is around 1.6, and the numerical value of maximum equivalent stress produced is around 72GPa.

From these numerical values of simulation results, it is found that the equivalent stress and equivalent strain acquired from simulation of cutting by a tool with negative and smaller rake angle are greater than those by a tool with greater rake angle. Besides, when the tools have the same rake angle, the equivalent stress and equivalent strain acquired from simulation of cutting by a round edge tool are greater than those by a sharp edge tool. The maximum equivalent stress and maximum equivalent strain acquired from cutting simulation by different cutting tools are summarized by the paper in Table 5. From Table 5, it is known that the maximum equivalent stress and maximum equivalent strain acquired from simulation of cutting by a tool with smaller rake angle are greater, and that the maximum equivalent stress and maximum equivalent strain acquired from simulation of cutting by the round edge tool with edge radius are greater than those by the sharp edge tool.

Table 5: Numerical values of maximum equivalent stress and maximum equivalent strain acquired from cutting simulation of perfect crystalline-lattice single-crystal copper material by four different diamond tools.

	Maximum equivalent Stress $\bar{\sigma}$ (GPa)	Maximum equivalent Stress $\bar{\epsilon}$
Round edge tool with rake angle 0°	71	1.5
Sharp edge tool with rake angle 0°	68	1.3
Round edge tool with rake angle 15°	65	1.2
Round edge tool with rake angle -15°	72	1.6

4.2.3 Analysis of temperature distribution of the cut workpiece

Using the abovementioned calculation method of heat source and temperature of the cut workpiece by applying the quasi-steady molecular statics nanocutting simulation model developed by this paper, this paper calculates the temperature produced from the plastic heat source and friction heat source on the cross-section near the center of the cut copper workpiece. When the cutting force is stable, this paper adds up the total temperature rise produced from the plastic heat source of copper workpiece material and the total temperature rise produced from the friction heat source. Their contour lines are further drawn out in order to present the temperature field distribution diagram on the cross-section near the center of the cut single-crystal copper workpiece.

The cutting simulation of this paper becomes more stable from the 12,000th step to the 18,000th step. Therefore, this paper takes the cutting in the 14,000th step to observe the temperature field distribution trend on the cross-section near the center of a single-crystal copper workpiece. Figure 13 shows the diagram of temperature field of a perfect-crystal copper workpiece cut by a round-edge tool with rake angle 0°, clearance angle 10° and edge radius 5Å. The highest temperature produced is around 783K. Figure 14 shows the diagram of temperature field of a perfect crystalline lattice copper workpiece cut by a sharp edge tool with rake angle 15° and clearance angle 10°. The highest temperature produced is around 762K. As known from Fig. 13 and Fig. 14, when the perfect crystalline lattice copper workpiece is being cut, the heat source temperature is concentrated on the chips in contact with the tip zone. Besides, higher temperature is produced from cutting by round edge tool than that by sharp edge tool; and the high-temperature zone is a little bit greater. This is possibly because the area of the round edge of tool is greater than the sharp edge of tool, so that the contact area of workpiece is also greater, and the cutting force, equivalent stress and equivalent strain of round edge tool are also greater during cutting. As a result, both the plastic deformation heat and friction heat are greater.

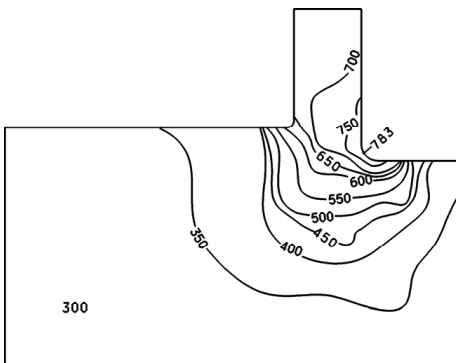


Figure 13: Diagram of temperature field of a perfect-crystal copper workpiece cut by a round-edge tool with rake angle 0°, clearance angle 10° and edge radius 5Å.

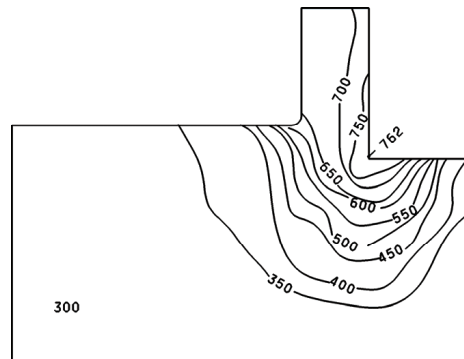


Figure 14: Diagram of temperature field of a perfect crystalline lattice copper workpiece cut by a sharp-edge tool with rake angle 0° and clearance angle 10°.

Figure 15 shows the diagram of temperature field of a perfect-crystal copper workpiece cut by a round-edge tool with rake angle 15°, clearance angle 10° and edge radius 5Å. The highest temperature produced is around 748K. Figure 16 shows the diagram of temperature field of a perfect crystalline lattice copper workpiece cut

by a round-edge tool with rake angle -15° and clearance angle 10° . The highest temperature produced is around 807K. As known from the figures from Fig. 13 to Fig. 16, when the perfect crystalline lattice copper workpiece is being cut, heat source temperature is concentrated on the chips in contact with the tip zone of tool. Besides, a cutting tool with negative rake angle or zero rake angle would produce higher temperature than the temperature produced by positive rake angle during cutting. Since the numerical values of cutting force, equivalent stress and equivalent strain of the machined workpiece cut by a tool with negative rake angle or zero rake angle are greater than those by a tool with positive rake angle, the plastic deformation heat and friction heat are thus led to be greater.

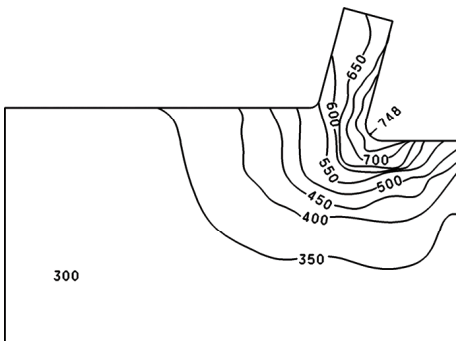


Figure 15: Diagram of temperature field of a perfect-crystal copper workpiece cut by a round-edge tool with rake angle 15° , clearance angle 10° and edge radius 5\AA .

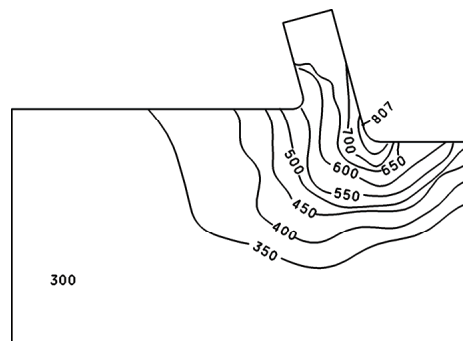


Figure 16: Diagram of temperature field of a perfect crystalline lattice copper workpiece cut by a round-edge tool with rake angle -15° and clearance angle 10° .

4.2.4 Analysis on the cut workpiece's temperature rise caused by plastic heat source and friction heat source, as well as analysis on friction force of workpiece atoms in contact with the tool face

This paper firstly calculates the Morse force of atoms on the cross-section near the center of workpiece in contact with the cutting tool, and then decomposes the Morse force to be the force in tangential direction along the tool face and the normal force vertical to the tool face. The force in tangential direction along the tool face is just the friction force during the contact between atoms and cutting tool. This paper takes the diagram of the cross-section near the center of workpiece in the $14,000^{\text{th}}$ step of cutting. And the calculated friction forces during contact of workpiece atoms with the tool face are listed out in a form by this paper for analysis.

Figure 17 (a) shows the diagram of the 14000th step's simulation result, and Fig. 17(b) shows the diagram of the cross-section near the center of a perfect-crystal copper workpiece nanocutting by a round edge tool with rake angle 0°, clearance angle 10° and edge radius 5Å. The numbered atoms in the figure are the workpiece atoms in contact with the tool face.

Table 6 shows the temperature rise ($\Sigma\Delta T_d$) caused by plastic heat source and temperature rise ($\Sigma\Delta T_w$) caused by friction heat source, as well as the total temperature rise ($\Sigma\Delta T$) of the cut copper workpiece atoms in the 14000th step of Fig. 17. As known from Table 6, for No. 3 atom, its temperature rise caused by plastic heat source is 438K, its temperature rise caused by friction heat source is 45K, and the total temperature rise is the greatest, around 483K. As it is mentioned before that the room temperature is 300K, thus the final temperature for No.3 atom is 783K in Table 6 shown. Table 7 shows the normal force, and friction force produced from the atoms in contact with the tool face in the 14000th step of Fig. 17. As known from Table 7, No. 3 atom has the greatest friction force, around 39.5nN. In Table 7, T is the calculated temperature rise of workpiece caused by friction force in the 14,000th step.

Figure 18(a) shows the diagram of the 14000th step's simulation result, and Fig. 18(b) shows the diagram of the cross-section near the center of a perfect-crystal copper workpiece cut by a sharp-edge tool with rake angle 0° and clearance angle 10°. As known from Table 8, for No. 3 atom, its temperature rise caused by plastic heat source is 421K, its temperature rise caused by friction heat source is around 41K, and the total temperature rise is the greatest, around 462K. As it is mentioned before that the room temperature is 300K, thus the final temperature for No.3 atom is 762K in Table 8 shown. Table 9 shows the normal force produced from the atoms in contact with the tool face in Fig. 18. As known from Table 9, No. 3 atom has the greatest friction force, around 32.1nN. As seen from the comparison of numerical values in Table 6 and Table 8, during cutting by a round-edge tool, the temperature rise of workpiece atoms produced by plastic heat source and friction heat source is greater than that during cutting by a sharper tool. And as seen from the comparison of numerical values in Table 7 and Table 9, the friction force of workpiece atoms during cutting by a round edge tool is greater than that during cutting by a sharper tool. Hence, the temperature rise T in the 14000th step caused by friction heat is also higher.

Figure 19(a) shows the diagram of the 14000th step's simulation result, and Fig. 19(b) shows the diagram of the cross-section near the center of a perfect-crystal copper workpiece cut by a round edge tool with rake angle 15°, clearance angle 10° and edge radius 5Å. The numbered atoms in the figure are the workpiece atoms in contact with the tool face. As known from Table 10, for No. 3 atom, its temperature

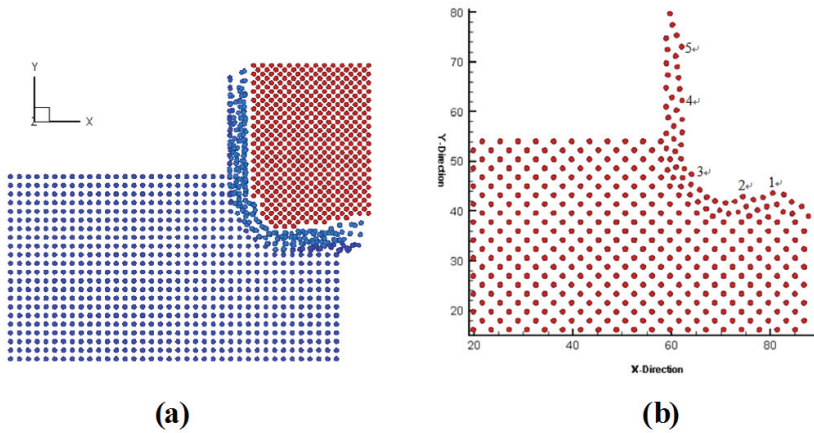


Figure 17: Diagram of (a) the 14,000th step's simulation result, and (b) the cross-section near the center, of a copper workpiece nanocut by a round-edge tool with rake angle 0° and clearance angle 10°.

Table 6: Temperature rise during cutting by a round-edge tool with rake angle 0°(only in the 14,000th step).

No. of atom	The total temperature rise by the plastic deformation heat $\Sigma\Delta T_d$ (K)	The total temperature rise by the frictional heat $\Sigma\Delta T_w$ (K)	The total temperature rise $\Sigma\Delta T$ (K)	The final temperature (K)
1	183	25	208	508
2	284	38	322	622
3	438	45	483	783
4	413	43	456	756
5	372	33	405	705

rise caused by plastic heat source is 421K, its temperature rise caused by friction heat source is around 36K, and the total temperature rise is the greatest, around 448K. As it is mentioned before that the room temperature is 300K, thus the final temperature for No.3 atom is 748K in Table 10 shown. Table 11 shows the normal force produced from the atoms in contact with the tool face and the friction force in tangential direction in Fig. 19. As known from Table 11, No. 3 atom has the greatest friction force, around 29.4nN.

Figure 20(a) shows the diagram of the 14000th step's simulation result, and Fig.20(b)

Table 7: Force, displacement and temperature rise produced by the atoms in contact with the tool face during cutting by a round-edge tool with rake angle 0° (in the $14,000^{th}$ step).

No. of atom	The displacement on the surface of the tool (\AA)	The normal force on the surface of the tool (nN)	The friction force on the surface of the tool (nN)	$T(K)$ in the 14000^{th} step
1	0.00200	26.544	13.455	0.136
2	0.00100	38.891	38.891	0.531
3	0.00400	29.670	39.560	1.121
4	0.00188	27.600	36.801	1.006
5	0.00400	26.675	22.344	0.305

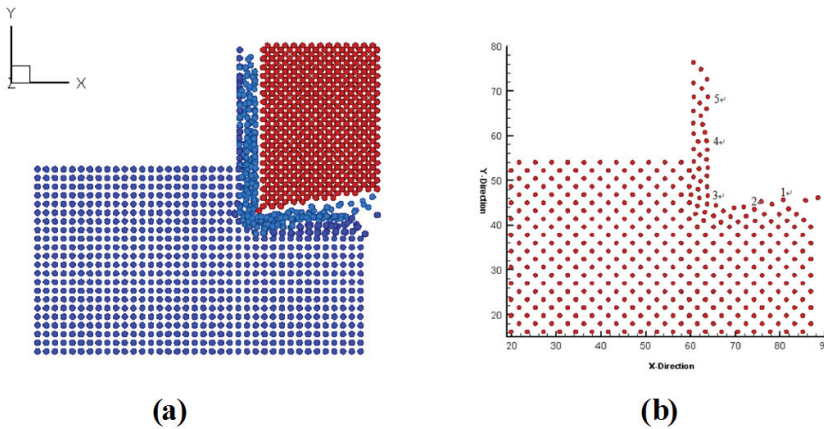


Figure 18: Diagrams of (a) the $14,000^{th}$ step's simulation result, and (b) the cross-section near the center, of a copper workpiece nanocut by a sharp-edge tool with rake angle 0° and clearance angle 10° .

shows the diagram of the cross-section near the center of a perfect-crystal copper workpiece cut by a sharp edge tool with rake angle 15° and clearance angle 10° . The numbered atoms in the figure are the workpiece atoms in contact with the tool face. As known from Table 12, for No. 3 atom, its temperature rise caused by plastic heat source is 463K, its temperature rise caused by friction heat source is around 44K, and the total temperature rise is the greatest, around 507K. As it is mentioned before that the room temperature is 300K, thus the final temperature for No.3 atom is 807K in Table 12 shown. Table 13 shows the normal force produced

Table 8: Temperature rise during cutting by a sharp tool with rake angle 0° (in the 14,000th step).

No. of atom	The total temperature rise by the plastic deformation heat $\Sigma\Delta T_d$ (K)	The total temperature rise by the frictional heat $\Sigma\Delta T_w$ (K)	The total temperature rise $\Sigma\Delta T$ (K)	The final temperature (K)
1	106	26	132	432
2	255	31	286	586
3	421	41	462	762
4	387	36	423	723
5	375	27	402	702

Table 9: Force, displacement and temperature rise produced by the atoms in contact with the tool face during cutting by a sharp-edge tool with rake angle 0° (only in the 14,000th step).

No. of atom	The displacement on the surface of the tool (\AA)	The normal force on the surface of the tool (nN)	The friction force on the surface of the tool (nN)	T (K) in the 14000 th step
1	0.00200	16.714	8.681	0.194
2	0.00210	20.714	12.681	0.243
3	0.00400	24.130	32.100	1.063
4	0.00135	22.043	30.387	0.586
5	0.00200	18.728	16.654	0.222

from the atoms in contact with the tool face and the friction force in tangential direction in Fig. 20. As known from Table 13, No. 3 atom has the greatest friction force, around 28.6nN.

As seen from the figures from Fig. 17 to Fig. 20, and from Table 6 to Table 13, during cutting by a cutting tool with negative or zero rake angle, the temperature increment of workpiece atoms produced from friction force and friction heat source is greater than the temperature produced by positive rake angle, and the greatest friction forces all happen to the places a little bit close to the area of tip zone. The total temperature rise by the plastic deformation heat ($\Sigma\Delta T_d$) is greater than the temperature rise by the frictional heat ($\Sigma\Delta T_w$), so in the nanoscale orthogonal cutting process, the main heat is produced from the plastic deformation heat.

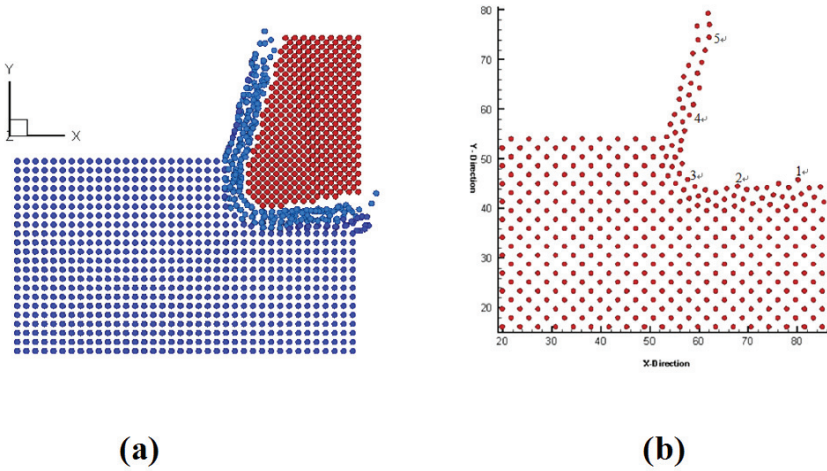


Figure 19: Diagrams of (a) the 14,000th step's simulation result, and (b) the cross-section near the center, of a copper workpiece nanocut by a round edge tool with rake angle 15°, clearance angle 10° and edge radius 5 Å.

Table 10: Temperature rise during cutting by a round edge tool with rake angle 15° (in the 14,000th step).

No. of atom	The total temperature rise by the plastic deformation heat $\Sigma\Delta T_d$ (K)	The total temperature rise by the frictional heat $\Sigma\Delta T_w$ (K)	The total temperature rise $\Sigma\Delta T$ (K)	The final temperature (K)
1	97	20	117	417
2	277	31	308	608
3	412	36	448	748
4	382	32	414	714
5	348	28	376	676

5 Conclusion

This paper uses three-dimensional quasi-steady molecular statics nanoscale orthogonal cutting model to carry out simulation of cutting of copper material in order to observe the effects caused by the use of sharp diamond tool and round edge diamond tools with different rake angles to cut perfect single-crystal copper material. This paper's employment of quasi-steady molecular statics is the use of the calculation method of the trajectory of each atom's coordinates in each step, to directly

Table 11: Force, displacement and temperature rise produced by the atoms in contact with the tool face during cutting by a round-edge tool with rake angle 15° (in the $14,000^{th}$ step)

No. of atom	The displacement on the surface of the tool (Å)	The normal force on the surface of the tool (nN)	The friction force on the surface of the tool (nN)	$T(K)$ in the 14000^{th} step
1	0.00026	22.056	5.910	0.061
2	0.00490	31.967	8.566	0.722
3	0.00193	28.669	29.445	0.960
4	0.00052	19.804	9.614	0.522
5	0.00238	22.062	5.911	0.080

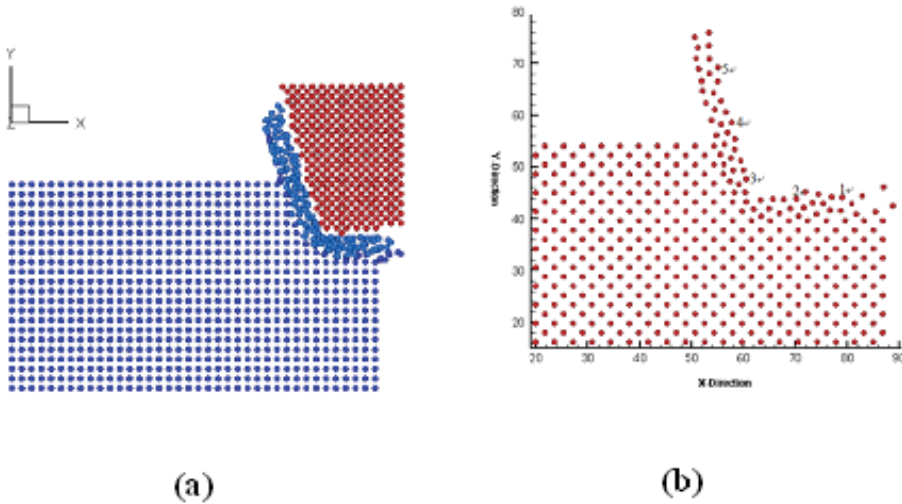


Figure 20: Diagrams of (a) the $14,000^{th}$ step's simulation result, and (b) the cross-section near the center, of a copper workpiece nanocut by a sharp-edge tool with rake angle -15° and clearance angle 10°

solve the force balance equations in X direction, Y direction and Z direction. This paper also uses straight-line search method that solves the function of several variables by engineering optimization, in order to fix the coordinates of the optimal displaced position of atoms. After that, according to the coordinate values of the displaced atoms, the nanoscale strain and stress are imported. This paper analyzes the trend of equivalent strain and equivalent stress. Further using the calculation method of heat source and temperature of the related cut workpiece by applying

Table 12: Temperature rise during cutting by a sharp tool with rake angle -15° (in the 14,000th step).

No. of atom	The total temperature rise by the plastic deformation heat $\Sigma\Delta T_d$ (K)	The total temperature rise by the frictional heat $\Sigma\Delta T_w$ (K)	The total temperature rise $\Sigma\Delta T$ (K)	The final temperature (K)
1	276	25	301	601
2	433	35	468	768
3	463	44	507	807
4	392	32	424	724
5	378	28	406	706

Table 13: Force, displacement and temperature rise produced by the atoms in contact with the tool face during cutting by a sharp tool with rake angle -15° (in the 14,000th step).

No. of atom	The displacement on the surface of the tool (\AA)	The normal force on the surface of the tool (nN)	The friction force on the surface of the tool (nN)	T (K) in the 14000 th step
1	0.00026	33.467	11.647	0.188
2	0.00122	38.867	38.543	0.983
3	0.00412	41.224	36.238	1.327
4	0.00423	14.533	30.006	0.876
5	0.00516	25.980	25.980	0.513

the quasi-steady molecular statics nanocutting simulation model developed by this paper, this paper calculates the temperature rise caused by the plastic heat source and friction heat source on the cross-section near the center of the cut copper workpiece material. After the temperature rise caused by these two heat sources is added up, the total temperature rise is resulted. For the result of temperature distribution calculated by this paper using molecular statics simulation, and the result of temperature distribution acquired from molecular dynamics simulation, their rough numerical values and qualitiveness are rather close. It can be seen that the simulation equation developed by the paper is feasible.

According to the above simulation results, the following conclusions are drawn:

1. Using diamond tools with four different edge shapes at the tip to carry out orthogonal cutting behavior of a perfect single-crystal copper workpiece would cause effect on cutting force. It is found that a round-edge tool has greater orthogonal

cutting force and thrust force than a sharp tool during cutting of workpiece, and the equivalent stress and equivalent strain produced are also greater. Using sharp diamond tool with rake angle of 0° and round-edge diamond tools with edge radius to cut copper material, this paper finds that the sharp tool and round-edge tools with negative or zero rake angles have greater orthogonal cutting force and thrust force during cutting of workpiece, and the equivalent stress and equivalent strain produced are also greater. The numerical values of orthogonal cutting force and thrust force acquired during cutting by a round edge diamond tool are greater than those acquired during cutting by a sharp diamond tool. This is because the contact area of the front tip of a round-edge tool with the workpiece is greater than that of a sharp tool, so that the affected atoms are more, and the accumulation of force is also greater. The chip shape is also different with the different edge shapes of cutting tools.

2. This paper explores how the orthogonal cutting act of perfect single-crystal copper material by diamond tools with four different edge shapes affects the heat source temperature of workpiece. Using a sharp diamond tool and a round-edge diamond tool with edge radius 5\AA , both having the same rake angle, for cutting, this paper finds that the round-edge tool produces greater heat source zone than the sharp tool during cutting of workpiece, and the highest temperature of workpiece is also greater. The highest temperature is concentrated on the workpiece chips in contact with tool tip zone. This paper also takes the round-edge diamond tools with rake angles from -15° to 15° and with edge radius 5\AA to carry out cutting. It is found that during cutting of workpiece, the highest temperature of workpiece cut by the sharp-edge tool and round-edge tool with negative rake angle (-15°) is greater than that cut by the sharp-edge diamond tool and round-edge diamond tool with edge radius 5\AA , both with greater rake angle (15°).

3. The numerical value of the highest temperature of workpiece acquired during cutting by a round edge diamond tool is greater than that by a sharp diamond tool. This is because heat source temperature comes from the plastic deformation heat source temperature and the friction heat source temperature produced from the friction force with tool face. The equivalent stress and strain as well as the cutting force and thrust force obtained during cutting by a round-edge tool are greater than the numerical values obtained by a sharp-edge tool. Besides, the greater the equivalent stress and strain, the greater the plastic heat source temperature; and cutting force and thrust force are the sum of Morse force of atoms. Therefore, the greater the Morse Force, the greater the friction force decomposed on the tool face; and the greater the friction force, the greater the friction heat source temperature. The temperature rise of plastic deformation heat is greater than the temperature rise of friction heat, so in the nanoscale orthogonal cutting process, the main heat is

produced from the plastic deformation heat.

Acknowledgement: The authors would like to give special thanks to the National Science Council, Taiwan, Republic of China, for financial support through Contract No. NSC 99-2221-E-011-019.

References

Shimada, S. (1990): Molecular Dynamics Analysis as Compared with Experimental Results of Micromachining. *Ann. CIRP* 117-120.

Childs, T. H. C.; Maewaka, K. (1990): Computer-aided Simulation and Experimental Studies of Chip Flow and Tool Wear in the Turning of Flow Alloy Steels by Cemented Carbide Tools. *Wear* 235-250.

Belak, J.; Stowers, I. F. (1990): A Molecular Dynamics Model of the Orthogonal Cutting Process. *Proc. Am. Soc., Prec. Eng.* 76-79.

Kim, J. D.; Moon, C. H. (1995): A study on microcutting for the configuration of tools using molecular dynamics. *Journal of Materials Processing Technology*: 309-314.

Fang, F.Z.; Wu, H.; Zhou, W.; Hu, X. T. (2007): A study on mechanism of nano-cutting single crystal silicon. *Journal of Materials Processing Technology*: 407-410.

Pei, Q.X.; Lu, C.; Fang, F.Z.; Wu, H. (2006): Nanometric cutting of copper: A molecular dynamics study. *Computational Materials Science*: 434- 441.

Inamura, T.; Takezawa, N. (1991): Cutting Experiments in a Computer Using Atomic Models of a Copper Crystal and a Diamond Tool. *Int. J. Japan Soc. Prec. Eng.*: 259-266.

Inamura, T.; Takezawa, N. (1992): Atomic-Scale Cutting in a Computer Using Crystal Models of Copper and Diamond. *Annals of the CIRP*: 121-124.

Ikawa, N ; Shimada, S ; Tanaka, H ; Ohmori, G.. (1991): An Atomistic Analysis of Nanometric Chip Removal as Affected by Tool-Work Interaction in Diamond Turning. *Annals of the CIRP*: 551-554.

Lin, Z. C.; Huang, J. C. (2004): A nano-orthogonal Cutting Model Based on a Modified Molecular Dynamics Technique. *Nanotechnology*: 510-519.

Lin, Z.C., Pan, W. C. and Lo, S. P., (1995) "A Study of Orthogonal Cutting with Tool Flank Wear and Sticking Behavior on the Chip-Tool Interface", *Journal of Materials Processing Technology*, Vol.52, No.2-4, pp.524-538.

Inamura, T.; Takezawa N.; Kumaki, Y. (1993): Mechanics and energy dissipation in nano scale cutting. *Annals. CIRP*: 79-82.

Cai, M. B.; Li, X. P.; Rahman, M. (2007): Study of the Temperature and Stress in Nanoscale Ductile Mode Cutting of Silicon Using Molecular Dynamics Simulation. *Journal of Materials Processing Technology*: 607–612.

Kwon, Y. W.; Jung, S. H. (2004): Atomic model and coupling with continuum model for static equilibrium problems. *Computational Structures Technology*: 1993-2000.

Igor, Ye; Telitchev; Oleg, Vinogradov (2006): A method for quasi-static analysis of topologically variable lattice structures. *International Journal of Computational Methods*: 71-81.

Jeng, Y. R.; Tan, C. M. (2004): Study of Nanoindentation Using FEM Atomic Model. *Journal of Tribology*: 767-774.

Rentsch, R.; Inasaki, I. (2006): Effects of Fluids on the Surface Generation in Material Removal Processes-Molecular Dynamics Simulation-. *Annals CIRP*: 601-604

Girifalco, L. A.; Weizer, V. G. (1959): Application of the Morse Potential Function to Cubic Metals. *Phys. Rev.*: 687-690.

Zhang, L.; Tanaka, H. (1997): Towards a deeper understanding of wear and friction on the atomic scale- a molecular dynamics analysis. *Wear*: 44-53.

Rau, J. S. (1999): *A Study on Mechanical Problems of Nanoscopic Micro-structures by Molecular Dynamics Theory*. Master Thesis, Department of Mechanical Engineering, National Cheng Kung University, Taiwan.